Optimal coordination and reorganization of photosynthetic properties in C_4 grasses

Haoran Zhou[1,2,3], Erol Akçay[1], Brent Helliker[1]

[1]Department of Biology, University of Pennsylvania, Philadelphia, PA 19104, USA

[2]School of the Environmental, Yale University, New Haven, CT 06511, USA

[3]University Corporation for Atmospheric Research, Boulder, CO 80301, USA

Correspondence: Haoran Zhou

Phone: 1-215-808-7042

Email: zhouhaoran06@gmail.com

ORCID iD: 0000-0002-5852-9535

Erol Akçay: eakcay@sas.upenn.edu

Brent Helliker: helliker@sas.upenn.edu

Running title: Optimal coordination in C_4 photosynthesis

Conflict of interest: None declared.

Paper type: Original Article

Word count: 5368

Number of figures: 7

Number of tables: 1

Supplementary material:

Supplementary Material I: supplementary dataset

Number of supplementary figures: 4

Number of supplementary tables: 11

Funding:

HZ and this research is supported by the NOAA Climate and Global Change Postdoctoral Fellowship Program, administered by UCAR's Cooperative Programs for the Advancement of Earth System Science (CPAESS) under award #NA18NWS4620043B and is also supported by the Dissertation Completion Fellowship provided by the Graduate Division of School of Arts and Sciences, University of Pennsylvania. BH is supported by NSF-IOS award 1856587.

Abstract

C_3 and C_4 are major functional types in terrestrial biosphere models, with photosynthesis traits as important input parameters. The evolution of C_4 required reorganizations of Calvin-Benson-cycle and coordination of C_4-cycle enzymes, resulting in divergences of physiological traits between C_3 and C_4. In addition, photosynthesis further optimized after the evolution of C_4 causing diversification within C_4 lineages due to different evolutionary histories. We combined optimality modeling, physiological measurements and phylogenetic analysis to examine how various aspects of C_4 photosynthetic machinery were reorganized and coordinated within C_4 lineages and as compared to closely-related C_3 in grasses. Optimality models and measurements indicated a higher maximal electron transport to maximal Rubisco carboxylation ratio (J_{max}/V_{cmax}) in C_4 than C_3, consistent with the optimal prediction to maximize photosynthesis. The coordination between Calvin-Benson and C_4 cycles (V_{pmax}/V_{cmax}), however, is in line with the optimal modeling results under 200 ppm, as opposed to current CO_2. Such inconsistencies can be explained by a slowly declining assimilation rate beyond optimal V_{pmax}/V_{cmax}. Although rapid coordination occurred early in C_4 evolution, C_4 is still under optimizing processes and photosynthetic measures have continued to increase across time. Lastly, better understandings of J_{max}/V_{cmax}, V_{pmax}/V_{cmax} and fluorescence-based-electron-transport proffer enhanced approaches to parameterize terrestrial biosphere models.

Key words C_4 photosynthesis, electron transport, grass, optimality, J_{max}/V_{cmax}, V_{pmax}/V_{cmax}, evolution

Introduction

C_3 and C_4 are major photosynthesis pathways and important functional types identified in the

terrestrial biosphere models, e.g., Earth System Models (ESMs) and Land Surface Models (LSMs) (Booth et al., 2012; Schaefer et al., 2012; Croft et al., 2017; Rogers et al., 2017). Photosynthetic traits and parameters of C_3 and C_4 photosynthesis, e.g., maximal Rubisco carboxylation rate (V_{cmax}) and maximal electron transport (J_{max}), are crucial inputs in these models. Such parameters, as well as the J_{max}/V_{cmax}, are well-documented for C_3 photosynthesis, however, the C_4 photosynthesis are still underrepresented currently due to lack of empirical reports and estimation (Bellasio *et al.*, 2016). The evolution of C_4 occurred over an extended period that encompassed many different climate change scenarios; therefore C_4 could respond to the future climate change differently than C_3 (Ward et al., 1999; Leakey et al., 2009; Wittmer et al., 2010; Morgan et al., 2011; Reich et al., 2018). Additionally, it has recently been proposed that by taking a lineage-based, or evolutionary, approach to ESM and LSM parameterization that a more realistic approach to functional diversity can be captured by these large-scale models (Griffith et al. 2020). Thus, it is crucial to identify the trait divergences of C_4 photosynthesis from C_3, especially with regard to the photosynthetic parameters.

C_4 photosynthesis evolved as a response to inefficiencies of C_3 photosynthesis that are exacerbated under certain environmental conditions: low CO_2, drought, high temperature and high light (Ehleringer & Monson, 1993; Ehleringer *et al.*, 1997; Edwards and Smith, 2010; Zhou et al., 2018). Rubisco, the CO_2 carboxylating enzyme of the Calvin-Benson (CB) cycle also assimilates O_2 as the first reaction of photorespiration and consequently reduces CB cycle efficiency up to 30% in C_3 species (Ehleringer *et al.*, 1991; Bauwe *et al.*, 2010; Raines 2011). The C_4 pathway concentrates CO_2 around Rubisco and dramatically reduces photorespiration by segregating atmospheric CO_2 uptake by Phosphoenolpyruvate carboxylase (PEPc) and CB-cycle into two compartments within the leaf. The operation of C_4

84 cycle does have additional ATP costs for which C_3 plants do not remunerate (Hatch, 1987).
85 In sum, the assembly of C_4 photosynthesis broke the balance between CO_2 carboxylation and
86 electron transport of the CB cycle, which existed in C_3 ancestors: C_4 photosynthesis elevates
87 the efficiency of CO_2 carboxylation at the expense of using more energy from electron
88 transport (Sage, 2001, 2004, 2016; Christin & Osborne, 2014; Lundgren *et al.*, 2019). Thus, a
89 further reorganization of resource allocation between Rubisco carboxylation and electron
90 transport and the coordination between CB and C_4 cycle should occur along with, or as a
91 consequence of, C_4 formation. Furthermore, selection optimized the function of the C_4
92 through intermediate steps through adjusting physiological traits (Christin & Osborne, 2014;
93 Sage, 2016) and different C_4 lineages evolved at different time points and endured different
94 evolutionary histories. We therefore expect diversification in photosynthetic traits and
95 parameters among C_4 lineages. If C_4 photosynthesis is continuously under extended
96 optimization after its formation (Edwards, 2019; Heyduk et al., 2019), such diversification
97 would also represent evolutionary trends between photosynthetic parameters and
98 evolutionary time/ages. In the current study, we examine how various aspects of C_4
99 photosynthetic machinery— nitrogen allocation between Rubisco carboxylation and electron
100 transport, and CB and C_4 cycle— were reorganized and coordinated within C_4 lineage, as
101 well as compared to closely-related C_3 species, and whether the coordination of C_4
102 machineries are on a walk toward or have already reached the optimal state.
103
104 The relative ratio among V_{cmax}, J_{max} and maximal PEP carboxylation rate (V_{pmax}) could
105 represent the coordination within CB cycle and between CB and C_4 cycles. The resource
106 allocation between the Rubisco carboxylation and electron transport is represented by
107 J_{max}/V_{cmax}. Although J_{max}/V_{cmax} has been empirically measured in numerous C_3 species
108 (Wullschleger, 1993) and examined with optimal modeling results of J_{max}/V_{cmax} for C_3

109 (Walker *et al.*, 2014; Kromdijk & Long, 2016; Quebbeman & Ramirez, 2016), there have
110 been far fewer measurements or predictions in C_4. The coordination among CB cycle and the
111 C_4 cycle could be represented by the relationships among V_{cmax}, J_{max} and V_{pmax}. As a
112 relationship between J_{max} and V_{cmax} has been established above, V_{pmax}/V_{cmax} could be taken
113 into consideration to depict a complete picture of the functional coordination (Yin *et al.*,
114 2016).
115
116 In C_3 plants J_{max}/V_{cmax} displays acclimation with changing environmental factors
117 (temperature, CO_2, light, and water availability; Onoda *et al.*, 2005; Rodriguez-Calcerrada *et*
118 *al.*, 2008; Kromdijk & Long, 2016; Yin *et al.*, 2018), and it is expected that J_{max}/V_{cmax} and
119 V_{pmax}/V_{cmax} might also vary in C_4. Sage and McKown (2006) proposed that C_4 may show less
120 plasticity and acclimation in phenotypical traits in response to global climate change, due to
121 their complex anatomical and biochemical features, e.g., the structural and physiological
122 integration of the mesophyll-bundle sheath complex. Combining theoretical predictions and
123 empirical examination of how J_{max}/V_{cmax} and V_{pmax}/V_{cmax} vary with environment could
124 elucidate the acclimation capability C_4 and further show if acclimation occurs in an optimal
125 manner. Such an understanding of C_4 responses to changing climate would reduce the
126 uncertainty of global carbon flux prediction (Beerling & Quick, 1995; Quebbeman &
127 Ramirez, 2016; Croft et al., 2017; Rogers et al., 2017).
128
129 In addition to the coordination between CB and C_4 cycle detailed above, we expect a
130 coordination between cyclic electron transport and total electron transport. Cyclic-electron
131 transport, which produces ATP only, has been proposed to be enhanced C_4 plants as
132 compared to C_3 plants to fulfill the extra ATP requirements of C_4 cycle (Takabayashi *et al.*,
133 2005; Nakamura et al., 2013; Munekage, 2016; Munekage & Taniguchi, 2016; Yin & Struik,

134 2018). Chlorophyll fluorescence has been widely used for C_3 species to estimate the J_{max} (Yin
135 et al., 2009; Bellasio et al., 2016); however, chlorophyll fluorescences, representing the
136 electron transport associated with linear electron transport, differs between C_3 and C_4 species.
137 Lack of details in the proportion of linear electron transport in total electron transport in C_4
138 species, therefore, hindered the use of fluorescence method to estimate electron transport in
139 C_4 species. We expected such a ratio will be lower in C_4 than that in C_3. Establishing this
140 ratio will provide for an additional tool to estimate J_{max} using fluorescence measurements, as
141 well as V_{cmax} and V_{pmax} for C_4 species.
142
143 In the current study, we first used physiological models coupling photosynthesis, hydraulics
144 and nitrogen stoichiometry to predict the optimal J_{max}/V_{cmax} and V_{pmax}/V_{cmax}. Then, we
145 performed in vivo experiments to estimate these parameters empirically on grass lineages
146 including C_3 and C_4 species selected from the PACMAD clade (Grass Phylogeny Working
147 Group II, 2012; Spriggs *et al.*, 2014) and compared these to published in vitro measurements.
148 By sampling multiple independent origins of C_4 species within a phylogenetic context
149 (Edwards *et al.*, 2007; Cavender-Bares *et al.*, 2009), we were able to use phylogenetic
150 comparative methods to examine the divergence of traits between C_3 and C_4 species and, to
151 detect whether there are continuous evolutionary trends. In sum, we used optimality
152 modeling, physiological measurements and evolutionary comparative methods to examine
153 evolutionary trends, the approach to optimality, and to gain a better formal understanding of
154 J_{max}/V_{cmax} and V_{pmax}/V_{cmax} in C_4 photosynthesis to reduce uncertainty in modeling the
155 carbon/nitrogen cycle, vegetation dynamics and productivity. Specifically, we aimed to test
156 and examine the following hypotheses and questions. (1) Reorganization in resource
157 allocation between Rubisco carboxylation and electron transport and coordination between
158 CB cycle and C_4 cycle in C_4 resulted in higher J_{max}/V_{cmax} and lower flr-ETR/J_{max} than C_3. (2)

C_4 values for J_{max}/V_{cmax} and V_{pmax}/V_{cmax} are optimized the for current environment conditions. (3) Although evolving millions of years ago, selection has continued to optimize C_4 after the evolution of the CCM, and this will yield a positive evolutionary trend between photosynthesis parameters and evolutionary age. (4) To examine the acclimation capability of C_4 species using predictions and measurements of how J_{max}/V_{cmax} and V_{pmax}/V_{cmax} vary with environmental change.

Materials and Methods

Plant material

We cultivated 35 closely related species, including nine C_3 and 26 C_4. The species belong to nine independent origins of closely-related C_3 and C_4 lineages. Detailed cultivation information is the same as Zhou *et al.* (2020).We, then, extracted the dated phylogenetic tree for the species from the dated phylogenetic trees (Spriggs *et al.*, 2014) (Fig. S1).

Physiological Modeling

Optimal J_{max}/V_{cmax} and V_{pmax}/V_{cmax} Based on the C_3 and C_4 models constructed in Zhou *et al.* (2018), which incorporates the soil-plant-air water continuum into traditional C_3 and C_4 photosynthesis models (Farquhar et al., 1980; von Caemmerer, 2000), we added stochiometric correlations between photosynthesis parameters and nitrogen. Using such a framework, we can model the optimal J_{max}/V_{cmax} and V_{pmax}/V_{cmax} simultaneously considering the following nitrogen stoichiometry:

The total nitrogen is the sum of different components (Evans, 1989):

$$N_{org} = N_P + N_E + N_R + N_S + N_O, \quad (1)$$

183 in which N_P represents the nitrogen in pigment proteins, N_E represents the nitrogen for the
184 electron transport system, N_R represents the nitrogen of Rubisco, N_S represents nitrogen in
185 soluble proteins except for Rubisco, and N_O represents additional organic leaf nitrogen not
186 invested in photosynthetic functions.
187 In order to model the optimal J_{max}/V_{cmax} and V_{pmax}/V_{cmax}, we need to consider the nitrogen
188 stoichiometry among J_{max}, V_{cmax} and V_{pmax}. We used empirical relationships found in previous
189 studies (Evans & Poorter, 2001; Niinemets & Tenhunen, 1997; Quebbeman & Ramirez,
190 2016):

191 $$N_P + N_E = 0.079 J_{max} + 0.0331\chi, \quad (2)$$

192 $$N_S = \nu J_{max}, \quad (3)$$

193 $$N_R = V_{cmax}/(6.25 \times V_{cr} \times \xi), \quad (4)$$

194 $$N_{PEP} = V_{pmax}/(6.72 \times V_{pr} \times \xi), \quad (5)$$

195 χ is the concentration of chlorophyll per unit area (μmol Chl m^{-2}), 0.079 is in mmol N s
196 $(\mu mol)^{-1}$, and 0.0331 is in mmol N $(\mu mol\ Chl)^{-1}$, $\nu \approx 0.3$ (mmol N s $(\mu\ mol)^{-1}$. V_{cr} is the
197 specific activity of Rubisco (the maximum rate of RuBP carboxylation per unit Rubisco; ≈
198 20.5 μmol CO_2 (g Rubisco)$^{-1}s^{-1}$) and 6.25 is grams RuBisCO per gram nitrogen in RuBisCO.
199 V_{pr} is the specific activity of PEPc, that is, the maximum rate of RuBP carboxylation per unit
200 PEPc (≈ 181.7 μmol CO_2 (g PEPC)$^{-1}s^{-1}$), 6.72 is grams PEPc per gram nitrogen in PEPC
201 (calculated from the amino acids composition of Fujita et al., 1984), and ξ is the mass in
202 grams of one millimole of nitrogen equal to 0.014 g N (mmol N)$^{-1}$.
203 Further, we simplify the equation (2) by assuming there is a coordination of resource
204 allocation between chlorophyll and electron transport for saturated light intensity, which
205 determines the J_{max}. We make this assumption for the light saturated condition and use the
206 empirical equation of Croft *et al.* (2017) to equation (2)

$$\chi = \frac{1000 J_{max}}{2.49} / \eta, \quad (6)$$

where η is the average molar mass for chlorophyll (900 g/mol). Thus,

$$N_{org} - N_O = 0.079 J_{max} + 0.0331\chi + \nu J_{max} + \frac{V_{cmax}}{6.25 \times V_{cr} \times \xi} + V_{pmax}/(6.72 \times V_{pr} \times \xi), \quad (7)$$

When the light intensity varies, the following function is used to adjust the electron transport rate (Ögren & Evans, 1993):

$$J = \frac{I_2 + J_{max} - \sqrt{(I_2 + J_{max})^2 - 4\Theta I_2 J_{max}}}{2\Theta}. \quad (8)$$

Also, all the photosynthetic parameters are temperature-sensitive (Zhou *et al.*, 2018).

In the optimal modeling processes, we set N_{org}- N_O as constant of 129 mmol N m^{-2} (which yield a V_{cmax}= 39 μmol m^{-2} s^{-1}, J_{max}= 195 μmol m^{-2} $s^{-1}$and V_{pmax}= 78 μmol m^{-2} s^{-1}, if assuming J_{max}/V_{cmax}=5 and V_{pmax}/V_{cmax}=2). Using these models, we modeled the assimilation rates with different J_{max}/V_{cmax} from 1 to 8 of 0.01 interval and different V_{pmax}/V_{cmax} from 0.5 to 5 of 0.01 to find the globally optimal assimilation rate with respect to both J_{max}/V_{cmax} and V_{pmax}/V_{cmax}. The corresponding J_{max}/V_{cmax} or J_{max}/V_{cmax} under the highest assimilation rates represent the optimal ratios. Then, we also model the locally optimal J_{max}/V_{cmax} and V_{pmax}/V_{cmax} when constraining the corresponding V_{pmax}/V_{cmax} and J_{max}/V_{cmax} with the average measured values respectively.

Using the model described above, we were able to model the optimal J_{max}/V_{cmax} and V_{pmax}/V_{cmax} under different environmental gradients: CO_2 of 200, 300, 400, 500 and 600 ppm; VPD and ψ_S of (0 MPa, 0.15) (0.625, -0.5), (1.25, -1), (1.875, -1.5), and (2.5, -2); light intensity of 2000, 1600, 1200, 800 and 400 μmol$m^{-2}s^{-1}$; temperature of 15, 20, 25, 30 and 35 °C. Since there is potential uncertainty for stochiometric relationships, we performed sensitivity analysis for the total nitrogen (from 100% to 50% with 10% interval of the regular nitrogen) for optimal J_{max}/V_{cmax} and V_{pmax}/V_{cmax} results and we also performed sensitivity

230 analysis for stoichiometry of PEPC by varying the $1/(6.72\times V_{pr} \times \xi)$ term in Eq. 5 from 50%
231 to 800%. For the C_3 pathway, all the modeling process are similar with the C_4 and a same
232 value of N_{org}- N_O is used, except that a simplified version of equation (7) is used as below
233 (Quebbeman & Ramirez, 2016):

234 $$N_{org} - N_O = 0.079J_{max} + 0.0331\chi + \nu J_{max} + \frac{V_{cmax}}{6.25\times V_{cr}\times\xi}, \quad (9)$$

235

236 ***Effects of decreasing V_{cmax}*** Using the model, we also simulated the effect of decreasing V_{cmax}
237 on the assimilation rate of both C_3 and C_4 pathway. In this modeling process, we hold J_{max}
238 and other photosynthetic parameters constant as the initial modeling condition as above, but
239 varying the V_{cmax} to 100%, 90%, 80%, 70%, 60% and 50% of the original values of C_3.
240

241 ***Gas exchange and fluorescence measurements***

242 We measured A/C_i curves using a LI-6400XT (LI-COR Inc., Lincoln, NE, USA) for all the
243 species by setting the CO_2 concentrations as 400, 200, 50, 75, 100, 125, 150, 175, 200, 225,
244 250, 275, 300, 325, 350, 400, 500, 600, 700, 800, 1000, 1200, 1400 ppm under light intensity
245 of 2000 $\mu molm^{-2}s^{-1}$. Data were recorded when the intercellular CO_2 concentration
246 equilibrated 2-5 minutes. Fluorescence was measured along with A/C_i curves using a 2 cm^2
247 fluorescence chamber head. After the change of CO_2 concentration, the quantum yield was
248 measured by multiphase flash when A reached a steady state (Bellasio *et al.*, 2014). The leaf
249 temperatures were controlled at 25°C, VPD varied at 1-1.7kPa and the flow rate of 500 μmol
250 s^{-1} for all the measurements. The cuvette was covered by Fun-Tak to lessen leakiness. We
251 used the estimation method in Zhou *et al.* (2019) for A/C_i curves to estimate in vivo V_{cmax},
252 J_{max}, and V_{pmax} with one slight methodological change. Since it is thought that the region of
253 V_{cmax} limit A/C_i is very narrow in C_4 species, we assigned the C_i regions limited by carbonic

254 anhydrase and V_{cmax} with a very low criteria of 5 Pa or below. We let the data points with C_i
255 ranging from 5 to 60 Pa CO_2 to be freely determined by which of the four potential
256 limitation states to minimize the estimation error. Using this method, we avoided the
257 potential bias of including optimal perspectives to the estimation method which could occur
258 when directly assigning the cross points co-limited by V_{cmax}, V_{pmax} and J_{max}. Fluorescence
259 results were used to calculate the flr-ETR (Genty *et al.*, 1989).
260
261 Furthermore, in vivo V_{cmax} estimated from A/C_i could be a source of uncertainty in C_4
262 species. In order to provide additional support to the measured J_{max}/V_{cmax} and V_{pmax}/V_{cmax}
263 value, we collected in vitro measured values for V_{cmax} and V_{pmax} from previous research,
264 which includes eleven studies with 87 averaged results reported under current and varying
265 environmental conditions (Supplementary Material I). Since it is impossible to obtain in vitro
266 J_{max} and the estimation of J_{max} from A/C_i curves is considered reliable, we also obtain the
267 corresponding A/C_i curves from these studies if they were reported, to obtain the J_{max}. The
268 combination of in vivo and in vitro measurements should yield a good representation of
269 current J_{max}/V_{cmax} and V_{pmax}/V_{cmax} states in the C_4 plants.
270
271 ***Chlorophyll measurements and leaf nitrogen***
272 Chlorophyll were measured using the spectrophotometer method (Porra *et al.*, 1989). We cut
273 the fresh leaves of species into pieces of 0.5 mm long (total leaf area was measured) and
274 submerged the fragments into DMF. After all the Chlorophyll was extracted and the leave
275 turned white, the supernatant was used to measure the absorption under 663.8 nm and 646
276 nm. Total Chlorophyll concentrations were calculated using the equation of Porra *et al.*
277 (1989). We measure leaf nitrogen contents for each sample using the CHNOS analyzer
278 (ECS4010, Costech Analytical Technologies, Inc., Valencia, CA).

279

280 ***Phylogenetic analysis***

281 We fitted each of the photosynthetic parameters (V_{cmax}, J_{max}, J_{max}/V_{cmax}, Total Chl, flr-
282 ETR/J_{max}, flr-ETR, V_{pmax} and V_{pmax}/V_{cmax}) to six different evolutionary models falling into
283 Brownian Motion model and Ornstein-Uhlenbeck Model using the R package of
284 "mvMORPH" (Table S1). The small-sample-size corrected version of Akaike information
285 criterion (AICc, the lower AICc, the better fit) and Akaike weights (AICw, the higher AICw,
286 the better fit) were used as criteria to figure out the best-fitted model. We used likelihood-
287 ratio test (LRT) method to test whether one model variant performs significantly better than
288 others and to determine whether there are significant differences between C_3 and C_4 species.
289 We also extract the evolutionary ages for each C_4 species from the dated phylogeny (Spriggs
290 *et al.*, 2014). We regressed the above photosynthetic traits with evolutionary ages to detect
291 potential evolutionary trends.

292

293 **Results**

294 ***In vivo and in vitro J_{max}/V_{cmax} follow the global optima in C_4, but V_{pmax}/V_{cmax} does not.***

295 In vivo and in vitro J_{max}/V_{cmax} are consistent with the optimal predictions under current CO_2
296 conditions, but V_{pmax}/V_{cmax} fell in to the optimal range under CO_2 of 200 ppm. The global
297 optima modelling results indicated maximal photosynthesis at the J_{max}/V_{cmax} of 5-6.2, which
298 is relatively constant across different CO_2 concentrations, while the optimal range for
299 V_{pmax}/V_{cmax} for C_4 species is 1.4-2.2 at CO_2 of 200 ppm, but decreases to 1-1.6 when CO_2
300 reaches 400 and 600 ppm (Fig. 1b, d, f). The averaged in vitro and in vivo J_{max}/V_{cmax} are
301 consistent with the global optimal predictions under CO_2 of 400 ppm (Fig. 1, Fig. 2a,
302 Supplementary Material I), as well as the locally optimal predictions controlling V_{pmax}/V_{cmax}
303 at the in vivo and in vitro level (Fig. 2). However, the averages of in vitro and in vivo

304 V_{pmax}/V_{cmax} are beyond the optimal predictions of global optima at CO_2 of 400 ppm, but the
305 measurement results are consistent with the optimal condition at CO_2 of 200 ppm (Fig. 1, 3,
306 4, S2, Supplementary Material I). The 3D images and the contour plots also illustrate that
307 when J_{max}/V_{cmax} is at the optimal range, beyond the optimal range of V_{pmax}/V_{cmax}, the
308 assimilation surface is quite flat: photosynthesis declines, but quite slowly; however, when
309 V_{pmax}/V_{cmax} drops outside of the optimal ranges, there are sharp decreases of photosynthesis
310 (Fig. 1). In vitro measurements indicated large variations of J_{max}/V_{cmax} and V_{pmax}/V_{cmax} at the
311 species level, and in vivo results, within a small scale of variation, fell completely into the
312 range of in vitro results (Fig. 2a and 3a).
313
314 ***C_4 species have higher J_{max}/V_{cmax} and lower* flr-ETR/J_{max} *than C_3 species.***
315 Phylogenetic analysis shows the J_{max}/V_{cmax} follows the Ornstein-Uhlenbeck model with a
316 higher stable state for C_4 species and a lower stable state for C_3 (Table 1; Fig. 1a). Such an
317 empirical relationship is consistent with the optimal modeling predictions for C_3 and C_4. We
318 looked further into how such a higher J_{max}/V_{cmax} in C_4 species is reached by comparing
319 individual empirical parameters. C_4 species has significantly higher stable states of J_{max}, but
320 significantly lower stable states of V_{cmax} and nitrogen content than their closely-related C_3
321 (Table 1). In order to examine the potential effects of decreasing V_{cmax} on assimilation rate,
322 we held the J_{max} as constant and changed the V_{cmax} from 100% to 50% of the original C_3
323 parameter values in the C_3 and C_4 models. A decrease in V_{cmax} will significantly decrease the
324 assimilation rates of C_3 species from 10 °C to 35°C under different CO_2 concentrations, while
325 decreasing V_{cmax} has little effects on the assimilation rates of C_4 species (Fig. 5).
326
327 The flr-ETR/ J_{max} was significantly higher in C_3 species than that in their closely related C_4
328 species, with the stable states of 1.08 and 0.64 for C_3 and C_4 respectively (Table 1).

329 Phylogenetic analysis indicated C_3 and C_4 species had the similar stable states of ETR, but C_4
330 has a higher total electron transport rate, J_{max} (Table 1).
331
332 ***The positive evolutionary trends of photosynthetic parameters***
333 Plotting the photosynthetic parameters with evolutionary ages, extracted from a dated
334 phylogeny for the multiple lineages, allows us to look for further evolutionary trends in C_4
335 and their closely related C_3 species. Regressions of evolutionary age versus photosynthetic
336 traits provide signals for long-term directional trends in photosynthetic machinery following
337 the establishment of C_4 photosynthesis (Fig. 6). A_{max}, J_{max}, total chlorophyll, V_{cmax} and V_{pmax}
338 showed significant positive correlations with evolutionary age in C_4 species, but not C_3
339 species, while nitrogen, J_{max}/V_{cmax}, V_{pmax}/V_{cmax} and flr-ETR/J_{max} did not show significant
340 correlation with the evolutionary age.
341
342 ***Optimal variation of J_{max}/V_{cmax} and V_{pmax}/V_{cmax} with environmental conditions.***
343 To understand how the J_{max}/V_{cmax} and V_{pmax}/V_{cmax} varied theoretically in response to
344 environmental changes (Fig. 7a, b, Fig. S3a, b), we calculated their optimal value for varying
345 CO_2 concentrations, water limitations, temperatures, and light intensities. The optimal
346 J_{max}/V_{cmax} is predicted to increase linearly in C_3 and, but increase a little bit and maintain
347 relatively constant in C_4 species with increasing CO_2 concentration (Fig. 7a). The optimal
348 J_{max}/V_{cmax} decreases similarly in both C_3 and C_4 species along with increasing water limitation
349 and increases similarly with decreasing light intensity and increasing temperatures (Fig. 7).
350 The changes of J_{max}/V_{cmax} with water limitation, light intensity, and temperature are non-
351 linear, with the rate-of-change increasing greatly after a threshold (water limitation of ψ_S=-1,
352 VPD=1.25, the light intensity of 800 μmol m^{-2} s^{-1} and temperature of 30 ^oC). The optimal
353 V_{pmax}/V_{cmax} decreases along with the increase of the CO_2 concentration, especially when CO_2

increases from 200 ppm to 300 ppm, but the change is little when CO_2 is above 400 ppm (Fig. 7c, S3c). However, V_{pmax}/V_{cmax} is relatively constant with the varying of water limitation conditions and light intensity (Fig. 7c,d, S3c,d). V_{pmax}/V_{cmax} decreases with the rise in temperature from 15 to 35 ^{o}C (Fig. 7d, S3d).

Sensitivity analysis for optimal J_{max}/V_{cmax} and V_{pmax}/V_{cmax}

Since there is a great variation of total nitrogen content in plants and there is uncertainty in the stoichiometry of PEPC, we performed sensitivity analysis and found the optimal modeling of J_{max}/V_{cmax} and V_{pmax}/V_{cmax} are robust. For C_3 photosynthesis, optimal J_{max}/V_{cmax} increases slightly with decreasing total nitrogen (7.7% increase of J_{max}/V_{cmax} with 50% reduction in total nitrogen), while for C_4, optimal J_{max}/V_{cmax} decreases with total nitrogen (16.2% increase of J_{max}/V_{cmax} with 50% reduction in total nitrogen) (Fig. S4a). The optimal V_{pmax}/V_{cmax} increases somewhat with decreasing total nitrogen (8.7% increase of V_{pmax}/V_{cmax} with 50% reduction in total nitrogen) (Fig. S4a). The optimal J_{max}/V_{cmax} is relatively constant with the change of stoichiometry of PEPC from 50% to 200%, but increases as the stoichiometry increases from 200% to 800% (Fig. S3b). The optimal V_{pmax}/V_{cmax} is relatively robust with the change of stoichiometry of PEPC.

Discussion

Our modeling efforts provide an explanation for the observed variation in J_{max}/V_{cmax} and V_{pmax}/V_{cmax}, and why V_{pmax}/V_{cmax} appears to be optimized for the lower bounds of atmospheric CO_2 of the Pleistocene. Our reported value of V_{pmax}/V_{cmax} are comparable with previous studies (Kubien *et al.*, 2003; Pengelly *et al.*, 2010; Yin *et al.*,2011, 2016; Pignon and Long, 2020), and two recent papers also indicated that the coordination between CB and C_4 cycles might represent a legacy of ancient low CO_2 conditions (Sundermann et al., 2018; Pignon and

379 Long, 2020). All extant C_4 species have gone through a low CO_2 bottleneck over the last 5
380 million years (Edwards et al., 2010). This bottleneck may have resulted in a strong selection
381 to increase V_{pmax}/V_{cmax} to maintain a high assimilation rate under the low CO_2 of glacial
382 maxima (~200 ppm). As CO_2 has risen, first with the beginning of the Holocene interglacial,
383 and then again with the continual burning of fossil fuels, V_{pmax}/V_{cmax} remained constant and
384 consequently exceeded the optimal V_{pmax}/V_{cmax} at higher CO_2. The effects of a too-high
385 V_{pmax}/V_{cmax} on assimilation rate are, however, minimal, thus the selection against increasing
386 V_{pmax}/V_{cmax} was likely weak. The explanation directly rests on the topology of assimilation
387 surface: when J_{max}/V_{cmax} and V_{pmax}/V_{cmax} are lower than the optimal states, assimilation rate
388 declines greatly; but when J_{max}/V_{cmax} and V_{pmax}/V_{cmax} exceed the optimal states, the decrease
389 of assimilation rate is minimal. Similarly, if a high J_{max}/V_{cmax} was selected for a given species
390 under, for example, growth at relatively low light conditions, the high J_{max}/V_{cmax} could well
391 be maintained for a long time even when moving to a high light environment. Such small
392 changes in assimilation rate may not change fitness enough to drive evolution toward optimal
393 states in natural plants; artificial selection and manipulation to change the J_{max}/V_{cmax} and
394 V_{pmax}/V_{cmax} toward the optimal states, however, might show potential in regard to increasing
395 total assimilation rate and productivity (Walker et al., 2018; Pignon and Long, 2020).
396
397 It has been hypothesized that after the evolution of the full C_4 CCM that selection across
398 various habitats would select for further physiologically optimal adjustments (Williams et al.,
399 2013; Stata et al., 2019); we find unequal support for such adjustments through time as
400 several physiological measures were positively related to evolutionary age, but there were no
401 trends with photosynthetic coordination. From this, we conclude that initially there was very
402 strong selection for coordination between the CB cycle, light reactions and the C_4 CCM, and
403 that changes in secondary or tertiary traits led to an increase in, for example, maximum CO_2

404 assimilation rate through time. Zhou et al. (2020) illustrated that hydraulic traits could be just
405 such an example of the secondary traits: the formation of C_4 pathway allowed for lower
406 stomatal conductance which triggered the decline of leaf hydraulic conductance and
407 capacitance over evolutionary time to further maximize the assimilation rate. Additionally,
408 anatomical organization within the leaf, like the ratio of mesophyll cells to bundle-sheath
409 cells, the 3D arrangement of cells and shifts in intercellular airspace could also be selected
410 upon through time towards a more optimal C_4 photosynthetic machine (Wang et al., 2017;
411 Alonso-Cantabrana et al., 2018; Edwards, 2019).
412
413 Higher J_{max}/V_{cmax} in C_4 than that in C_3 indicated a change in resource allocation, namely
414 nitrogen, between the light reactions and the CB cycle, and as a crucial evolutionary step for
415 elevating C_4 efficiency, it is important to look at how the reallocation may have occurred and
416 the larger-scale consequences. The modeling results indicate that a decrease of Rubisco
417 content is favored in C_4, because overall nitrogen requirements decrease and such a reduction
418 has minimal effects on net assimilation rate. Significantly lower V_{cmax} in all of our C_4 species
419 and lower Rubisco in previous studies confirmed the assertion (Brown, 1978; Ku *et al.,* 1979;
420 Sage and Pearcy, 1987; Sharwood *et al.*, 2016). Any surplus nitrogen not invested in Rubisco
421 could be distributed among three broad categories: 1) reallocated to the light reactions or 2)
422 stored or used to construct new tissues or 3) simply not taken up from the growth
423 environment, thus reducing total plant nitrogen requirements. Tissue *et al.* (1995) and
424 Ghannoum *et al.* (2010) detected lower Rubisco content and higher chlorophyll and thylakoid
425 content, supporting resource reallocation from RuBP carboxylation to electron transport
426 within the leaf. Our measurements provide evidence that the coordination of J_{max}/V_{cmax}
427 resulted from a mix of hypotheses 1) and 3). The significantly higher J_{max} and lower V_{cmax} in
428 C_4 than their closely-related C_3 species supports a reallocation of hypothesis 1). In addition,

429 hypothesis 3) likely occurred together with hypothesis 1) because C_4 species have
430 significantly lower nitrogen content. Hypothesis 2), not exclusive to hypotheses 1) and 3),
431 could be supported by evidence that C_4 plants maintain larger leaf areas (Ripley *et al.*, 2008).
432 These hypotheses are connected to potential ecological ramifications. Firstly, in a nitrogen-
433 depleted habitat, C_4 could have a competitive advantage as confirmed by Ripley *et al.* (2008;
434 although Sage & Pearcy, 1987, found no evidence for this). In habitats where nitrogen is not
435 limiting, the excess nitrogen could be used to construct more leaf area (Sage & Pearcy, 1987;
436 Anten *et al.*, 1995; Ripley *et al.*, 2008), and greater leaf area in the early stages of growth was
437 indeed seen by Atkinson *et al.* (2016). On the other hand, the lack of nitrogen reallocation
438 from the CB cycle to the light reactions may indicate physiological constraints in fertile
439 habitats. For example, photorespiration in C_3 plants is proposed to enhance the nitrate
440 metabolism (Oaks, 1994; Rachmilevitch *et al.*, 2004; Bauwe *et al.*, 2010; Bloom, 2015),
441 therefore the formation of CCM, which inhibits photorespiration, may reduce overall plant-
442 available nitrogen for C_4. In addition, the increase of J_{max} in C_4 is due to an enhanced cyclic
443 electron transport, while maintaining the linear electron transport at the same level of C_3.
444 Elevating cyclic electron transport is therefore a potentially important step in engineering C_4
445 photosynthesis into C_3 crops.
446
447 Empirical evidence indicates adaptive plasticity (or acclimation) of C_4 photosynthetic
448 coordination occurs under different environmental conditions, consistent with optimal
449 predictions. Contrary to what Sage and McKown (2006) proposed, C_4 exhibited significant
450 acclimation capability with varying CO_2 (Pinto et al. 2014; Pinto et al. 2016), water
451 availability (Sharwood et al. 2014), light intensity (Sharwood et al. 2014; Pengelly et al.
452 2010; Sonawane, 2016) and temperature (Sonawane, 2016; Pittermann and Sage 2001;
453 Kubien and Sage 2004; Serrano-Romero and Cousins, 2020) in both J_{max}/V_{cmax} and

454 V_{pmax}/V_{cmax} (Supplementary Material I). The varying trends in J_{max}/V_{cmax} are generally
455 consistent between the empirical measurements and optimal modeling predictions in the
456 current study: higher resource allocation to electron transport under shade, elevated CO_2,
457 high water availability and higher temperature. However, C_3 and C_4 species might respond
458 differently to environmental variations, especially in response to CO_2 variation shown in the
459 optimal modeling results. The V_{pmax}/V_{cmax} exceededs the optimal prediction when acclimated
460 to the current environmental conditiona, perhaps because V_{pmax}/V_{cmax} is constraint by a legacy
461 of acclimation to historical CO_2. These acclimation responses should be considered and
462 included in ESMs and LSMs to predict responses of C_3 and C_4 ecosystems to future climate
463 change (Rogers et al., 2017; Smith and Keenan, 2020).
464
465 Our improved estimates of J_{max}/V_{cmax}, V_{pmax}/V_{cmax} and flr- ETR/J_{max} for C_4 plants could
466 directly benefit terrestrial biosphere models. Although J_{max}, V_{cmax} and V_{pmax} are key input
467 parameters in global-scale models (Beerling & Quick, 1995; Zaehle *et al.*, 2005; Bonan *et al.*,
468 2011; Walker *et al.*, 2014), it is difficult and perhaps not feasible to measure all parameters
469 for numerous sites. If one the ratioed parameters described here, either J_{max}/V_{cmax}, V_{pmax}/V_{cmax}
470 and/or flr- ETR/J_{max}, is obtained then other parameters could be estimated. Using J_{max}/V_{cmax},
471 V_{pmax}/V_{cmax} and flr- ETR/J_{max} is especially crucial in C_4 species because in vivo estimation of
472 V_{cmax} and V_{pmax} are more difficult and less reliable, and in vitro measurements are not easily
473 performed over broad taxonomic or spatial scales. Our results suggest a value of around 5.5
474 for J_{max}/V_{cmax} and a value of 2 for V_{pmax}/V_{cmax} supported by optimality modeling and
475 empirical measurements. With an empirical value of around 60% found in the current study,
476 the measurement of flr- ETR could provide another tool to further estimate J_{max}, V_{cmax} and
477 V_{pmax}. Previous theoretical analysis also inferred values of flr- ETR/J_{max} of 60% and 50% in
478 C_4 (Yin et al., 2011; Yin & Struik, 2012; Yin & Struik, 2018).

The evolution of C_4 photosynthesis required the reorganization and coordination of the CB-cycle, the light reactions and the PEPc-based CCM. Strong divergence in J_{max}/V_{cmax} between C_4 and C_3 species indicates the resource allocation changes between light reactions and the CB cycle that were necessary to support the enhanced ATP requirement of the C_4 CCM (Osborn & Sack, 2012; Zhou et al., 2018). Observed J_{max}/V_{cmax} were within the predicted optimal zone suggesting that the resource reallocation between Rubisco carboxylation and electron transport are operating near optimality under current environmental conditions; however, the long tail exceeding the optimal J_{max}/V_{cmax} in empirical measurements indicates multiple species have over-allocated to electron transport, perhaps a legacy of native ecological conditions. The coordination between CB and C_4 cycles was in line with the optimal conditions under 200 ppm representing an over-allocation of resources for current environmental conditions, but there is little costs to assimilation rate due to this lack of optimality. Rapid coordination occurred early in C_4 evolution, but it appears that C_4 photosynthesis is still under selection for further optimization. The enhanced understanding of the evolution-based photosynthetic reorganization and coordination in C_4 photosynthesis, along with our ratio-based approach to obtain photosynthetic parameters can lead to a better parameterization of terrestrial biosphere models for C_4.

Acknowledgements

We sincerely thank Dr. Matteo Detto (Princeton University) for his help in building the optimal models for J_{max}/V_{cmax}.

Reference

Alonso-Cantabrana H., Cousins A.B., Danila F., Ryan T., Sharwood R.E., von Caemmerer S., Furbank R.T. (2018). Diffusion of CO_2 across the mesophyll-bundle sheath cell interface in a C_4 plant with genetically reduced PEP carboxylase activity. *Plant Physiology*, 178, 72–81.

Anten N.P., Schieving F., Medina E., Werger M.J.A., Schuffelen P. (1995). Optimal leaf area indices in C_3 and C_4 mono-and dicotyledonous species at low and high nitrogen availability. *Physiologia plantarum*, 95, 541-550.

Atkinson R.R., Mockford E.J., Bennett C., Christin P.A., Spriggs E.L., Freckleton R.P., Thompson K., Rees M., Osborne C.P. (2016). C_4 photosynthesis boosts growth by altering physiology, allocation and size. *Nature Plants*, 2, 16038.

Bauwe H., Hagemann M., Fernie A.R. (2010). Photorespiration: players, partners and origin. *Trends in plant science*, 15, 330-336.

Beerling D.J., Quick W.P. (1995). A new technique for estimating rates of carboxylation and electron transport in leaves of C_3 plants for use in dynamic global vegetation models. *Global Change Biology*, 1, 289-294.

Bellasio C., Beerling D.J., Griffiths H. (2016). An Excel tool for deriving key photosynthetic parameters from combined gas exchange and chlorophyll fluorescence: theory and practice. *Plant, cell & environment*, 39, 1180-1197.

Bellasio C., Burgess S.J., Griffiths H., Hibberd J.M. (2014). A high throughput gas exchange screen for determining rates of photorespiration or regulation of C_4 activity. *Journal of experimental botany*, 65, 3769-3779.

Bloom A.J. (2015). Photorespiration and nitrate assimilation: a major intersection between plant carbon and nitrogen. *Photosynthesis Research*, 123, 117-128.

Bonan G.B., Lawrence P.J., Oleson K.W., Levis S., Jung M., Reichstein M., Lawrence D.M., Swenson S.C. (2011). Improving canopy processes in the Community Land Model version 4 (CLM4) using global flux fields empirically inferred from FLUXNET data. *Journal of Geophysical Research: Biogeosciences*, 116(G2).

Booth B.B., Jones C.D., Collins M., Totterdell I.J., Cox P.M., Sitch S., Huntingford C., Betts R.A., Harris G.R. and Lloyd J. (2012). High sensitivity of future global warming to land carbon cycle processes. *Environmental Research Letters*, 7, p.024002.

Brown R.H. (1978). A difference in N use efficiency in C_3 and C_4 plants and its implications in adaptation and evolution 1. *Crop Science*, 18, 93-98.

von Caemmerer S. (2000). Biochemical models of photosynthesis. In Techniques in Plant Sciences. CSIRO Publishing, Colingwood, Australia, pp 91–122.

Cavender-Bares J., Kozak K.H., Fine P.V., Kembel S.W. (2009). The merging of community ecology and phylogenetic biology. *Ecology letters*, 12, 693-715.

Christin P.A., Osborne C.P. (2014). The evolutionary ecology of C_4 plants. *New Phytologist*, 204, 765-781.

Croft H., Chen J.M., Luo X., Bartlett P., Chen B., Staebler R.M. (2017). Leaf chlorophyll content as a proxy for leaf photosynthetic capacity. *Global change biology*, 23, 3513-3524.

Edwards E.J. (2019). Evolutionary trajectories, accessibility and other metaphors: the case of C4 and CAM photosynthesis. *New Phytologist*, 223, 1742-1755.

Edwards E.J., Osborne C.P., Strömberg C.A.E., Smith S.A., C_4 Grasses Consortium. (2010). The origins of C_4 grasslands: integrating evolutionary and ecosystem science. *Science*, 328, 587–591.

Edwards E.J., Still C.J., Donoghue M.J. (2007). The relevance of phylogeny to studies of global change. *Trends in Ecology & Evolution*, 22, 243-249.

Ehleringer J.R., Cerling T.E., Helliker B.R. (1997). C_4 photosynthesis, atmospheric CO_2, and climate. *Oecologia*, 112, 285-299.

Ehleringer J.R., Monson R.K. (1993). Evolutionary and ecological aspects of photosynthesis pathway variation. *Annual Review of Ecology and Systematics*, 24, 411-439.

Ehleringer J.R., Sage R.F., Flanagan L.B., Pearcy R.W. (1991). Climate change and the evolution of C_4 photosynthesis. *Trends in ecology & evolution*, 6, 95-99.

Evans J.R. (1989). Partitioning of nitrogen between and within leaves grown under different irradiances. *Functional Plant Biology*, 16, 533–548, doi:10.1071/PP9890533.

Evans J., Poorter H. (2001). Photosynthetic acclimation of plants to growth irradiance: the relative importance of specific leaf area and nitrogen partitioning in maximizing carbon gain. *Plant, Cell & Environment*, 24, 755-767.

Farquhar G.D., Von Caemmerer S., Berry J.A. (1980). A biochemical model of photosynthetic carbon dioxide assimilation in leaves of 3-carbon pathway species. *Planta*, 149, 78–90.

Fujita N., Miwa T., Ishijima S., Izui K., Katsuki H. (1984). The primary structure of phosphoenolpyruvate carboxylase of Escherichia coli. Nucleotide sequence of the ppc gene and deduced amino acid sequence. *The Journal of Biochemistry*, 95, 909-916.

Genty B., Briantais J.M., Baker N.R. (1989). The relationship between the quantum yield of photosynthetic electron transport and quenching of chlorophyll fluorescence. *Biochimica et Biophysica Acta (BBA)-General Subjects*, 990, 87-92.

572 Ghannoum O., Evans J.R., von Caemmerer S. (2010). Nitrogen and water use efficiency of
573 C_4 plants. In: C_4 photosynthesis and related CO_2 concentrating mechanisms (eds.
574 Raghavendra, A.S. & Sage, R.F.). Springer Science, The Netherlands, Dordrecht, pp.
575 129–146.
576 Grass Phylogeny Working Group II. 2012. New grass phylogeny resolves deep evolutionary
577 relationships and discovers C_4 origins. *New Phytologist*, 193, 304-312.
578 Griffith D.M., Osborne C.P., Edwards E.J., Bachle S., Beerling D.J., Bond W.J., Gallaher
579 T.J., Helliker B.R., Lehmann C.E., Leatherman L. and Nippert J.B. (2020). Lineage-
580 based functional types: characterising functional diversity to enhance the representation
581 of ecological behaviour in Land Surface Models. *New Phytologist*, 228, 15-23.
582 Hatch M.D. (1987). C_4 photosynthesis: a unique blend of modified biochemistry, anatomy
583 and ultrastructure. *Biochimica et Biophysica Acta (BBA)-Reviews on Bioenergetics*, 895,
584 81-106.
585 Heyduk K., Moreno-Villena J.J., Gilman I.S., Christin P.A., and Edwards E.J. 2019. The
586 genetics of convergent evolution: insights from plant photosynthesis. *Nature Review*
587 *Genetics*, 20, 485-493.
588 Kromdijk J., Long S.P. (2016). One crop breeding cycle from starvation? How engineering
589 crop photosynthesis for rising CO_2 and temperature could be one important route to
590 alleviation. *Proceedings of the Royal Society B: Biological Sciences*, 283, p.20152578.
591 Ku M.S.B., Schmitt M.R., Edwards G.E. (1979). Quantitative determination of RuBP
592 carboxylase-orygenase protein in leaves of several C_3 and C_4 plants. *Journal of*
593 *experimental botany*, 114, 89–98.
594 Kubien D.S., von Caemmerer S., Furbank R.T., Sage R.F. (2003). C_4 photosynthesis at low
595 temperature. A study using transgenic plants with reduced amounts of Rubisco. *Plant*
596 *Physiology*, 132, 1577-1585.
597 Kubien D.S., Sage R.F. (2004). Low-temperature photosynthetic performance of a C_4 grass
598 and a co-occurring C_3 grass native to high latitudes. *Plant, Cell & Environment*, 27, 907-
599 916.
600 Leakey A.D. (2009). Rising atmospheric carbon dioxide concentration and the future of C_4
601 crops for food and fuel. *Proceedings of the Royal Society B: Biological Sciences*, 276,
602 2333-2343. doi: 10.1098/rspb.2008.1517
603 Lundgren M.R., Dunning L.T., Olofsson J.K., MorenoVillena J.J., Bouvier J.W., Sage T.L.,
604 Khoshravesh R., Sultmanis S., Stata M., Ripley B.S., Vorontsova M.S. (2019). C_4
605 anatomy can evolve via a single developmental change. *Ecology letters*, 22, 302-312.

Morgan J.A., LeCain D.R., Pendall E., Blumenthal D.M., Kimball B.A., Carrillo Y., Williams D.G., Heisler-White J., Dijkstra F.A., and West M. (2011). C_4 grasses prosper as carbon dioxide eliminates desiccation in warmed semi-arid grassland. *Nature,* 476, 202-206. doi: 10.1038/nature10274.

Munekage Y.N. (2016). Light harvesting and chloroplast electron transport in NADP-malic enzyme type C_4 plants. *Current opinion in plant biology*, 31, 9-15.

Munekage Y.N., Taniguchi Y.Y. (2016). Promotion of cyclic electron transport around photosystem I with the development of C_4 photosynthesis. *Plant and Cell Physiology*, 57, 897-903.

Nakamura N., Iwano M., Havaux M., Yokota A., Munekage Y.N. (2013). Promotion of cyclic electron transport around photosystem I during the evolution of NADP–malic enzyme-type C_4 photosynthesis in the genus *Flaveria*. *New Phytologist*, 199, 832-842.

Niinemets Ü., Tenhunen J.D. (1997). A model separating leaf structural and physiological effects on carbon gain along light gradients for the shade-tolerant species *Acer saccharum*. *Plant Cell & Environment*, 20, 845–866.

Oaks A. (1994). Efficiency of nitrogen utilization in C_3 and C_4 cereals. *Plant Physiology*, 106: p.407.

Ögren E., Evans J.R. (1993). Photosynthetic light-response curves. *Planta*, 189, 182-190.

Onoda Y., Hikosaka K., Hirose T. (2005). The balance between RuBP carboxylation and RuBP regeneration: a mechanism underlying the interspecific variation in acclimation of photosynthesis to seasonal change in temperature. *Functional Plant Biology*, 32, 903-910.

Osborne C.P., Sack L. (2012). Evolution of C_4 plants: a new hypothesis for an interaction of CO_2 and water relations mediated by plant hydraulics. *Philosophical Transactions of the Royal Society B: Biological Sciences*, 367, 583-600.

Pengelly J.J., Sirault X.R., Tazoe Y., Evans J.R., Furbank R.T., von Caemmerer S. (2010). Growth of the C_4 dicot *Flaveria bidentis*: photosynthetic acclimation to low light through shifts in leaf anatomy and biochemistry. *Journal of experimental botany*, 61, 4109-4122.

Pignon C.P., Long S.P. (2020). Retrospective analysis of biochemical limitations to photosynthesis in 49 species: C_4 crops appear still adapted to pre-industrial atmospheric [CO2]. *Plant, Cell & Environment*, 43, 2606-2622.

Pinto H., Powell J.R., Sharwood R.E., Tissue D.T., Ghannoum O. (2016). Variations in nitrogen use efficiency reflect the biochemical subtype while variations in water use

efficiency reflect the evolutionary lineage of C_4 grasses at inter-glacial CO_2. *Plant, cell & environment*, 39, 514-526.

Pinto H., Sharwood R.E., Tissue D.T., Ghannoum O. (2014). Photosynthesis of C_3, C_3–C_4, and C_4 grasses at glacial CO_2. *Journal of Experimental Botany*, 65, 3669-3681.

Pittermann J., Sage R.F. (2001). The response of the high altitude C_4 grass *Muhlenbergia montana* (Nutt.) AS Hitchc. to long-and short-term chilling. *Journal of Experimental Botany*, 52, 829-838.

Porra R.J., Thompson W.A., Kriedemann P.E. (1989). Determination of accurate extinction coefficients and simultaneous equations for assaying chlorophylls a and b extracted with four different solvents: verification of the concentration of chlorophyll standards by atomic absorption spectroscopy. *Biochimica et Biophysica Acta (BBA)-Bioenergetics*, 975, 384-394.

Quebbeman J.A., Ramirez J.A. (2016). Optimal allocation of leaf-level nitrogen: Implications for covariation of V_{cmax} and J_{max} and photosynthetic downregulation. *Journal of Geophysical Research: Biogeosciences*,121, 2464-2475.

Rachmilevitch S., Cousins A.B., Bloom A.J. (2004). Nitrate assimilation in plant shoots depends on photorespiration. *Proceedings of the National Academy of Sciences*, 101, 11506-11510.

Raines C.A. (2011). Increasing photosynthetic carbon assimilation in C_3 plants to improve crop yield: current and future strategies. *Plant physiology*, 155, 36-42.

Reich P.B., Hobbie S.E., Lee T.D., Pastore M.A. (2018). Unexpected reversal of C_3 versus C_4 grass response to elevated CO_2 during a 20-year field experiment. *Science*, 360, 317-320. doi: 10.1126/science.aas9313

Ripley B.S., Abraham T.I., Osborne C.P. (2008). Consequences of C_4 photosynthesis for the partitioning of growth: a test using C_3 and C_4 subspecies of *Alloteropsis semialata* under nitrogen-limitation. *Journal of experimental botany*, 59, 1705-1714.

Rogers A., Medlyn B.E., Dukes J.S., Bonan G., Von Caemmerer S., Dietze M.C., Kattge J., Leakey A.D., Mercado L.M., Niinemets Ü., Prentice I.C. (2017). A roadmap for improving the representation of photosynthesis in Earth system models. *New Phytologist*, 213, 22-42. doi: 10.1111/nph.14283

Rodriguez-Calcerrada J., Reich P.B., Rosenqvist E., Pardos J.A., Cano F.J., Aranda I. (2008). Leaf physiological versus morphological acclimation to high-light exposure at different stages of foliar development in oak. *Tree physiology*, 28, 761-771.

Sage R.F. 2001. Environmental and evolutionary preconditions for the origin and diversification of the C_4 photosynthetic syndrome. *Plant Biology*, 3, 202–213.

Sage R.F. (2004). The evolution of C_4 photosynthesis. *New Phytologist*, 161, 341–370.

Sage R.F. (2016). Tracking the evolutionary rise of C_4 metabolism. *Journal of experimental botany*, 67, 2919-2922.

Sage R.F., McKown A.D. (2006). Is C_4 photosynthesis less phenotypically plastic than C_3 photosynthesis? *Journal of experimental botany*, 57, 303-317.

Sage R.F., Pearcy R.W. (1987). The nitrogen use efficiency of C_3 and C_4 plants: I. Leaf nitrogen, growth, and biomass partitioning in Chenopodium album (L.) and *Amaranthus retroflexus* (L.). *Plant Physiology*, 84, 954-958.

Schaefer K., Schwalm C.R., Williams C., Arain M.A., Barr A., Chen J.M., Davis K.J., Dimitrov D., Hilton T.W., Hollinger D.Y., Humphreys E. (2012). A model-data comparison of gross primary productivity: Results from the North American Carbon Program site synthesis. *Journal of Geophysical Research: Biogeosciences*, 117(G3).

Serrano-Romero, E.A., Cousins, A.B. (2020). Cold acclimation of mesophyll conductance, bundle-sheath conductance and leakiness in *Miscanthus× giganteus*. *New Phytologist* 226, 1594-1606.

Sharwood R.E., Sonawane, B.V., Ghannoum O. (2014). Photosynthetic flexibility in maize exposed to salinity and shade. *Journal of Experimental Botany*, 65, 3715-3724.

Sharwood R.E., Ghannoum O., Whitney S.M. (2016). Prospects for improving CO_2 fixation in C_3-crops through understanding C_4-Rubisco biogenesis and catalytic diversity. *Current Opinion in Plant Biology*, 31, 135-142.

Smith N.G., Keenan T.F. (2020). Mechanisms underlying leaf photosynthetic acclimation to warming and elevated CO_2 as inferred from least-cost optimality theory. *Global Change Biology*, 26, 5202-5216.

Sonawane, B.V. (2016). Environmental regulation of CO_2 concentrating mechanisms in C_4 grasses with different biochemical subtypes (Doctoral dissertation, Western Sydney University (Australia)).

Spriggs, E.L., Christin, P.A. and Edwards, E.J. (2014). C_4 photosynthesis promoted species diversification during the Miocene grassland expansion. *Plos one*, 9, p.e97722.

Stata M., Sage T.L., Sage R.F. (2019). Mind the gap: the evolutionary engagement of the C_4 metabolic cycle in support of net carbon assimilation. *Current Opinion in Plant Biology*, 49, 27-34. doi: 10.1016/j.pbi.2019.04.008

Sundermann E., Lercher M. and Heckmann D. (2018). Modeling Cellular Resource Allocation Reveals Low Phenotypic Plasticity of C_4 Plants and Infers Environments of C_4 Photosynthesis Evolution. bioRxiv (Preprint). Available at doi: https://doi.org/10.1101/371096 (Accessed April 15, 2020).

Takabayashi A., Kishine M., Asada K., Endo T., Sato F. (2005). Differential use of two cyclic electron flows around photosystem I for driving CO_2-concentration mechanism in C_4 photosynthesis. *Proceedings of the National Academy of Sciences*, 102, 16898-16903.

Tissue D.T., Griffin K.L., Thomas R.B., Strain B.R. (1995). Effects of low and elevated CO_2 on C_3 and C_4 annuals. II. Photosynthesis and leaf biochemistry. *Oecologia*, 101, 21-28.

Walker A.P., Beckerman A.P., Gu L., Kattge J., Cernusak L.A., Domingues T.F., Scales J.C., Wohlfahrt G., Wullschleger S.D., Woodward F.I. (2014). The relationship of leaf photosynthetic traits–V_{cmax} and J_{max}–to leaf nitrogen, leaf phosphorus, and specific leaf area: a meta-analysis and modeling study. *Ecology and evolution*, 4, 3218-3235.

Walker B.J., Drewry D.T., Slattery R.A, VanLoocke A., Cho Y.B., Ort D.R. (2018). Chlorophyll can be reduced in crop canopies with little penalty to photosynthesis. *Plant Physiology*, 176, 1215-1232.

Wang S., Tholen D., and Zhu X.G. (2017). C_4 photosynthesis in C_3 rice: a theoretical analysis of biochemical and anatomical factors. *Plant, cell & environment*, 40, 80-94.

Ward J.K., Tissue D.T., Thomas R.B., Strain B.R. (1999). Comparative responses of model C_3 and C_4 plants to drought in low and elevated CO_2. *Global Change Biology* 5: 857-867.

Williams B.P., Johnston I.G., Covshoff S., Hibberd J.M. (2013). Phenotypic landscape inference reveals multiple evolutionary paths to C_4 photosynthesis. *Elife*, 2, p.e00961. doi: 10.7554/eLife.00961

Wittmer M.H., Auerswald K., Bai Y., Schaeufele R., Schnyder H. (2010). Changes in the abundance of C_3/C_4 species of Inner Mongolia grassland: evidence from isotopic composition of soil and vegetation. *Global Change Biology*, 16, 605-616. doi: 10.1111/j.1365-2486.2009.02033.x

Wullschleger S.D. (1993). Biochemical limitations to carbon assimilation in C_3 plants - A retrospective analysis of the A/C_i curves from 109 species. *Journal of Experimental Botany*, 44, 907-920.

Yin X., Van Der Putten P.E., Driever S.M., Struik P.C. (2016). Temperature response of bundle-sheath conductance in maize leaves. *Journal of experimental botany*, 67, 2699-2714.

Yin X., Schapendonk A.H., Struik P.C. (2018). Exploring the optimum nitrogen partitioning to predict the acclimation of C_3 leaf photosynthesis to varying growth conditions. *Journal of experimental botany*, 70, 2435-2447.

Yin X., Struik P.C. (2012). Mathematical review of the energy transduction stoichiometries of C_4 leaf photosynthesis under limiting light. *Plant, cell & environment*, 35, 1299-1312.

Yin X., Struik P.C. (2018). The energy budget in C_4 photosynthesis: insights from a cell-type-specific electron transport model. *New Phytologist*, 218, 986-998.

Yin X., Struik P.C., Romero P., Harbinson J., Evers J.B., Van Der Putten P.E., Vos J.A.N. (2009). Using combined measurements of gas exchange and chlorophyll fluorescence to estimate parameters of a biochemical C_3 photosynthesis model: a critical appraisal and a new integrated approach applied to leaves in a wheat (*Triticum aestivum*) canopy. *Plant, Cell & Environment*, 32, 448-464.

Yin X., Sun Z., Struik P.C., Van der Putten P.E., Van Ieperen W.I.M., Harbinson J. (2011). Using a biochemical C_4 photosynthesis model and combined gas exchange and chlorophyll fluorescence measurements to estimate bundle-sheath conductance of maize leaves differing in age and nitrogen content. *Plant, cell & environment*, 34, 2183-2199.

Zaehle S., Sitch S., Smith B., Hatterman F. (2005). Effects of parameter uncertainties on the modeling of terrestrial biosphere dynamics. *Global Biogeochemical Cycles* 19: GB3020.

Zhou H, Akçay E, Helliker BR. 2019. Estimating C_4 photosynthesis parameters by fitting intensive A/C_i curves. *Photosynthesis research*, 141, 181-194.

Zhou H., Helliker B.R., Huber M., Dicks A., Akçay E. (2018). C_4 photosynthesis and climate through the lens of optimality. *Proceedings of the National Academy of Sciences*, 115, 12057-12062.

Zhou H., Akçay E., Edwards E., and Helliker B.R. (2020). The legacy of C_4 evolution in the hydraulics of C_3 and C4 grasses. bioRxiv. doi: https://doi.org/10.1101/2020.05.14.097030.

Table 1 Phylogenetic results of the best-fitted models and their parameters for photosynthesis parameters (summarizing Table S2-S10).

Property	Model	Model type	AICw	Root	
				C_3	C_4
J_{max}/V_{cmax}	Model 6*	OU	1.000	1.59	5.90
V_{cmax}	Model 6*	OU	0.769	59.52	23.03
J_{max}	Model 6*	OU	0.583	88.94	132.16
Total Chl	Model 1	BM	0.293	0.36	
flr-ETR/J_{max}	Model 5*	OU	1.000	1.08	0.64
Chl a/b	Model 5	OU	0.995	3.40	4.61
flr-ETR	Model 1	BM	**0.397**	88.94	
V_{pmax}	Model 4	OU	0.854	41.52	
V_{pmax}/V_{cmax}	Model 4	OU	0.875	1.97	
N	Model 5*	OU	0.562	3.62	2.53

If the values for C_3 and C_4 were different, it meant there were significant different values for C_3 and C_4 species (the evolutionary model with two different values of the root fit significantly better than the evolutionary model with the similar root).

Figures

Fig. 1 Modeling results of assimilation rate with respect to maximal electron transport to maximal Rubisco carboxylation (J_{max}/V_{cmax}) and maximal PEP carboxylation to maximal Rubisco carboxylation (V_{pmax}/V_{cmax}) under CO_2 concentration of 200, 400 and 600 ppm. Other environmental conditions are soil water potential (ψ_s)=-0.5 MPa, VPD=0.625, temperature of 25 °C and light intensity of 2000 μmol m^{-2} s^{-1}. Left: 3D plot; right: corresponding contour plot.

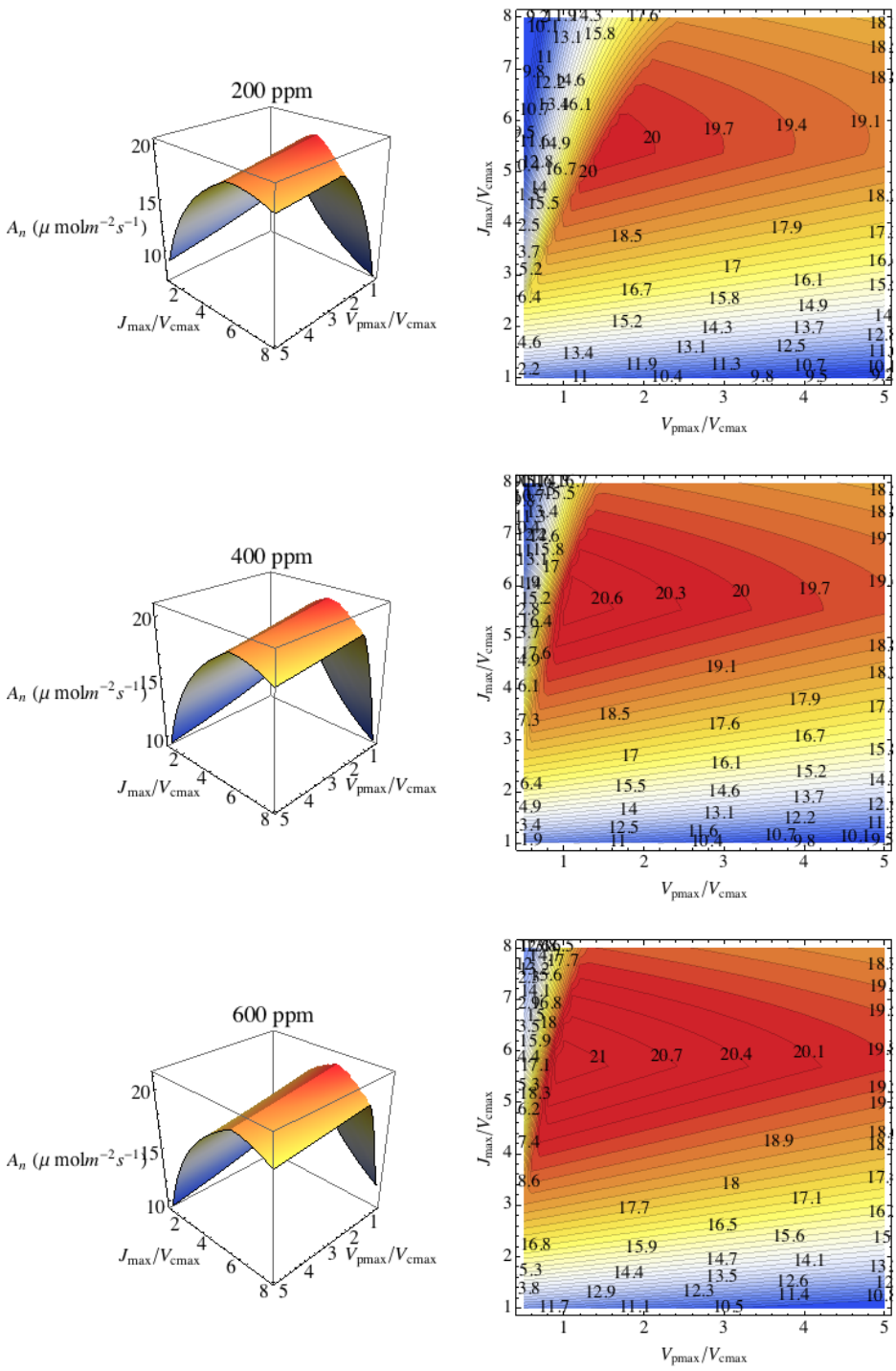

779

Fig. 2 Empirical measurements (a) and optimal modeling results (b) of J_{max}/V_{cmax} for C_3 and C_4 under ψ_S=-0.5 MPa, VPD=0.625, temperature of 25 °C and light intensity of 2000 μmol m^{-2} s^{-1}, the cultivating environmental condition. In (b), the black line represents C_3, solid red line represents C_4 modeling results with controlling V_{pmax}/V_{cmax} at the in vivo measurement level, dashed red line represents C_4 modeling results with controlling V_{pmax}/V_{cmax} at the in vitro measurement level.

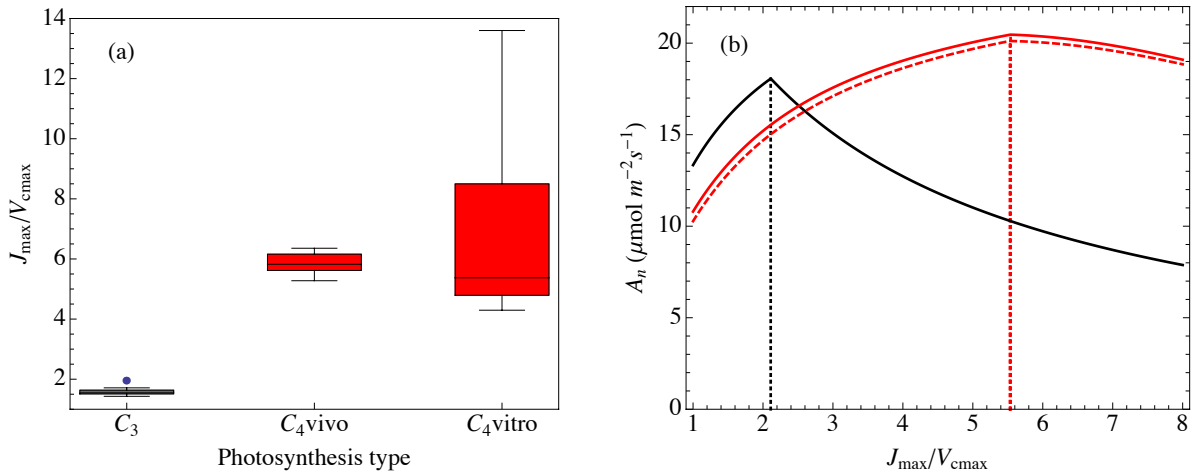

Fig. 3 Empirical measurements (a) and optimal modeling results (b) of V_{pmax}/V_{cmax} for C_4 under ψ_S=-0.5 MPa, VPD=0.625, temperature of 25 °C and light intensity of 2000 μmol m^{-2} s^{-1}, the cultivating environmental condition. In (b), solid red line represents C_4 modeling results with controlling J_{max}/V_{cmax} at the in vivo measurement level, dashed red line represents C_4 modeling results with controlling J_{max}/V_{cmax} at the in vitro measurement level.

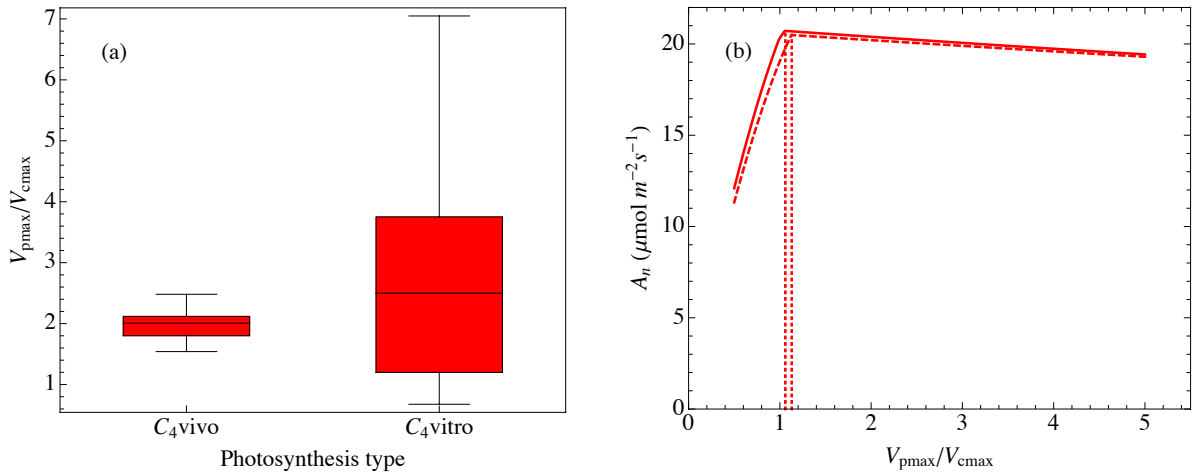

Fig. 4 Modeling results of assimilation rate with varying J_{max}/V_{cmax} and V_{pmax}/V_{cmax} for C_4 under different CO_2 concentration and ψ_S=-1MPa, VPD=1.25, temperature of 25 °C and light intensity of 2000 μmol m^{-2} s^{-1}, the common grassland growth condition. Modeling results were obtained by controlling the other parameter at the in vivo measurement level.

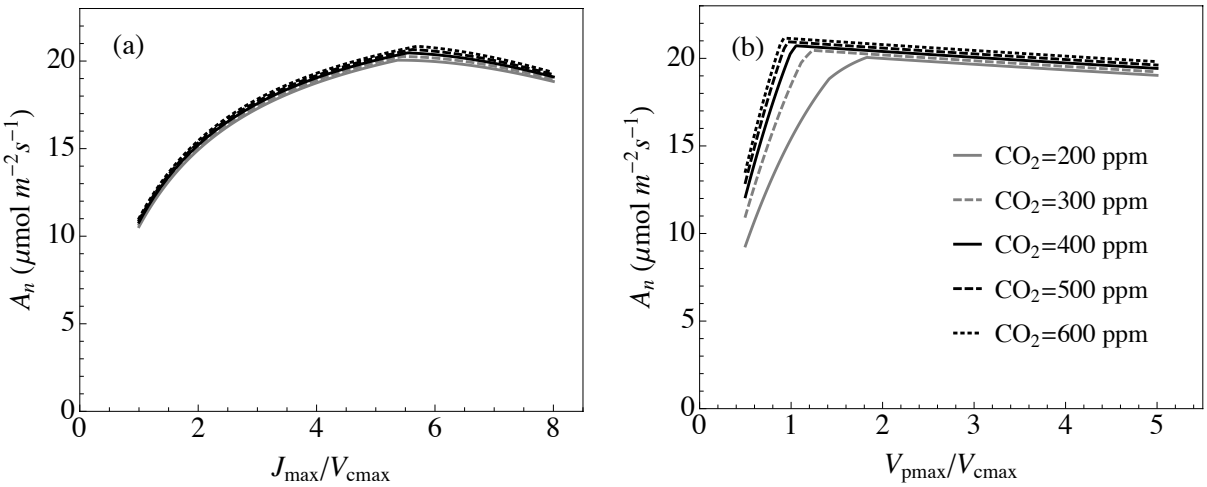

Fig. 5 Modeling results of changing V_{cmax} on assimilation rates for C_3 (acd) and for C_4 (bdf) under different CO_2. Solid black line: the initial modeling condition of V_{cmax} (a typical C_3 value of 69 μmol m^{-2} s^{-1}); dashed black line: 90% of the initial V_{cmax}; dotted black line: 80% of the initial V_{cmax}; solid grey line: 70% of the initial V_{cmax}; dashed grey line: 60% of the initial V_{cmax}; dotted grey line: 50% of the initial V_{cmax}.C_3 and C_4 parameters shared similar parameters except for the carbon concentration mechanism and different hydraulic conductance to mimic the initial origin of C_4 (see Zhou et al (2020) for other parameters).

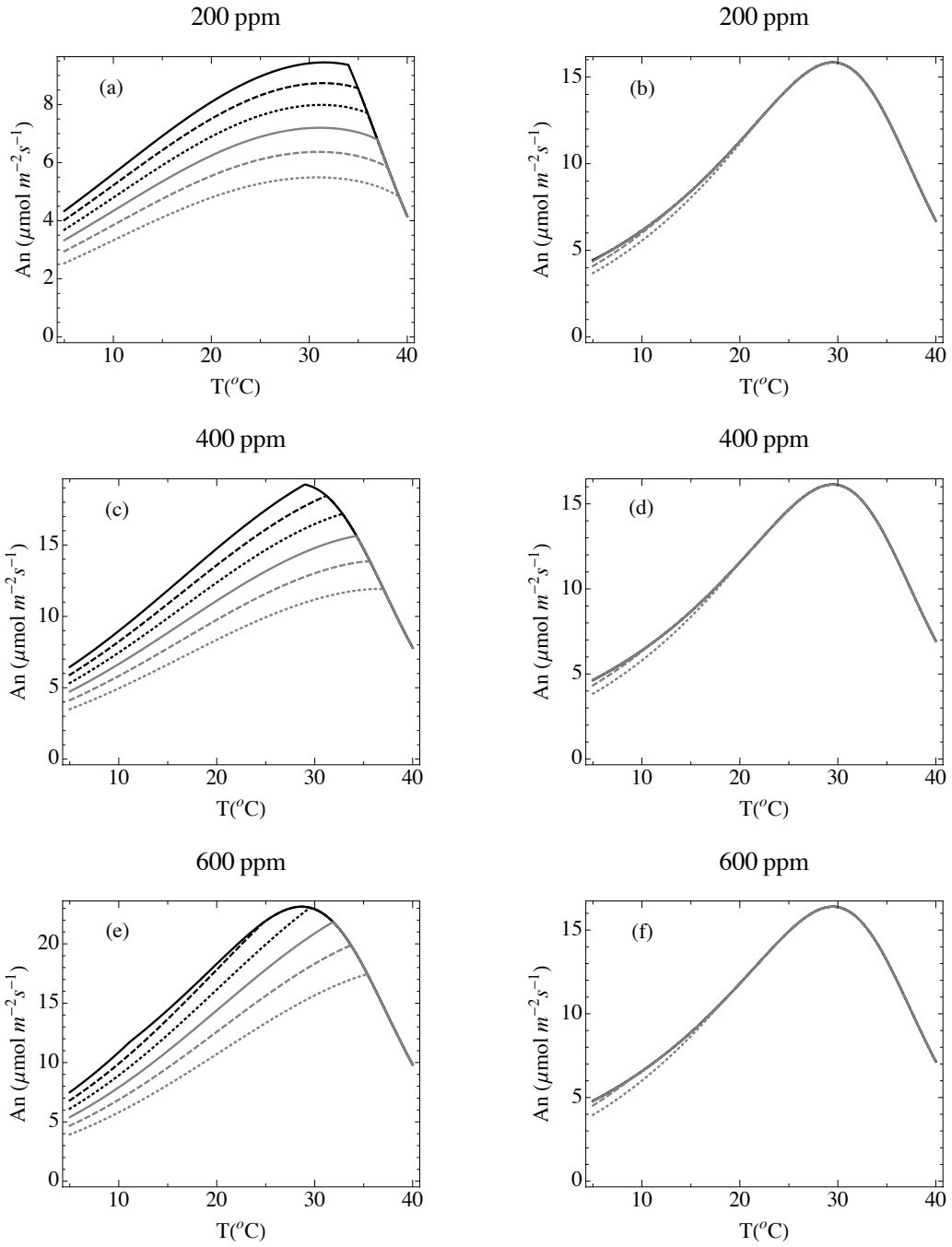

Fig. 6 The regression for maximal assimilation rate (A_{max}), J_{max}, total cholorophyll (Total chl), V_{cmax}, V_{pmax}, nitrogen concentration, J_{max}/V_{cmax}, V_{pmax}/V_{cmax} and fluorescence-estimated electron transport to J_{max} (ETR/ J_{max}) vs. the evolutionary age for the nine origins to show the evolutionary trend within C_4 (red) and within their closely-related C_3 species (black).

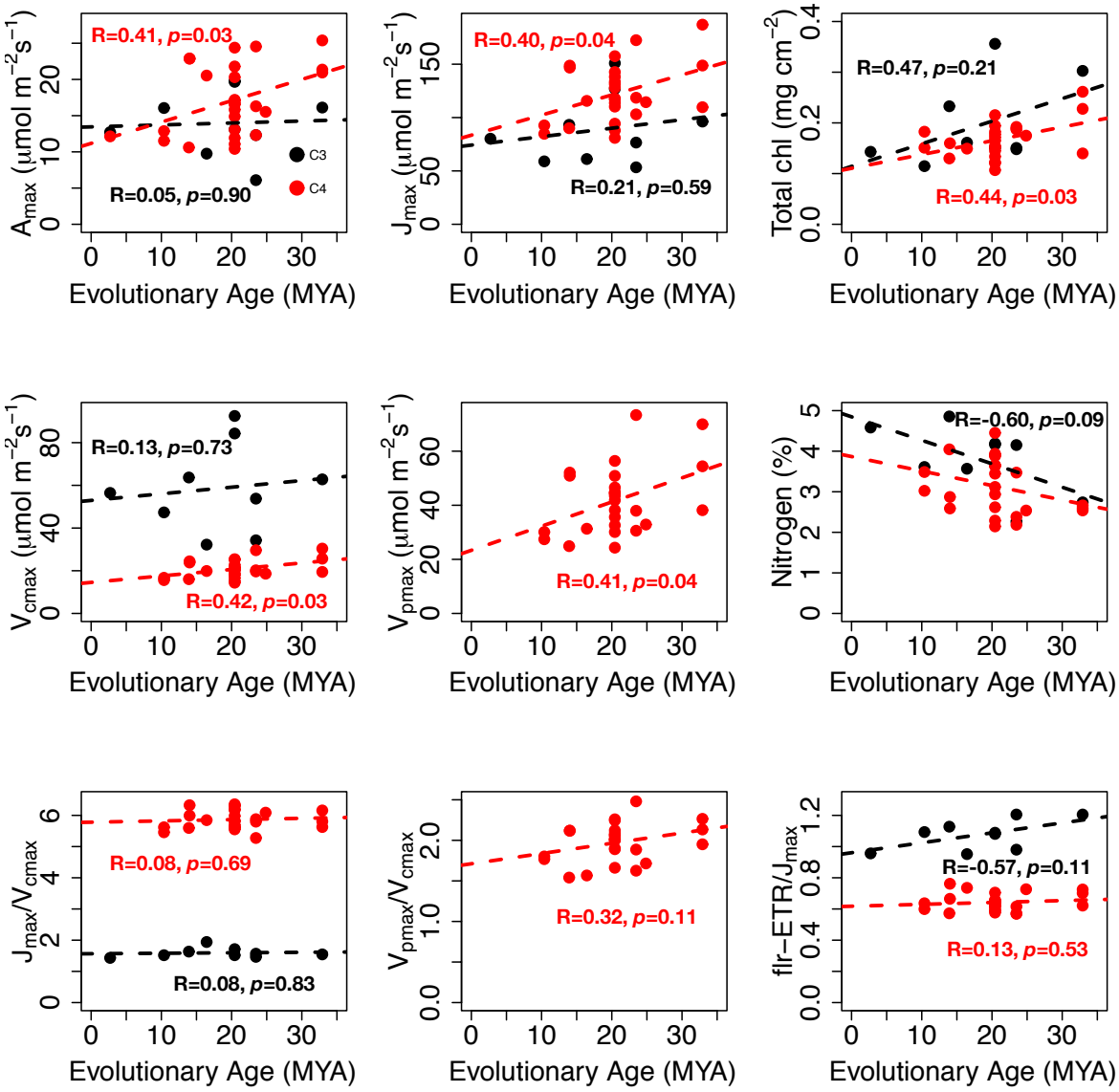
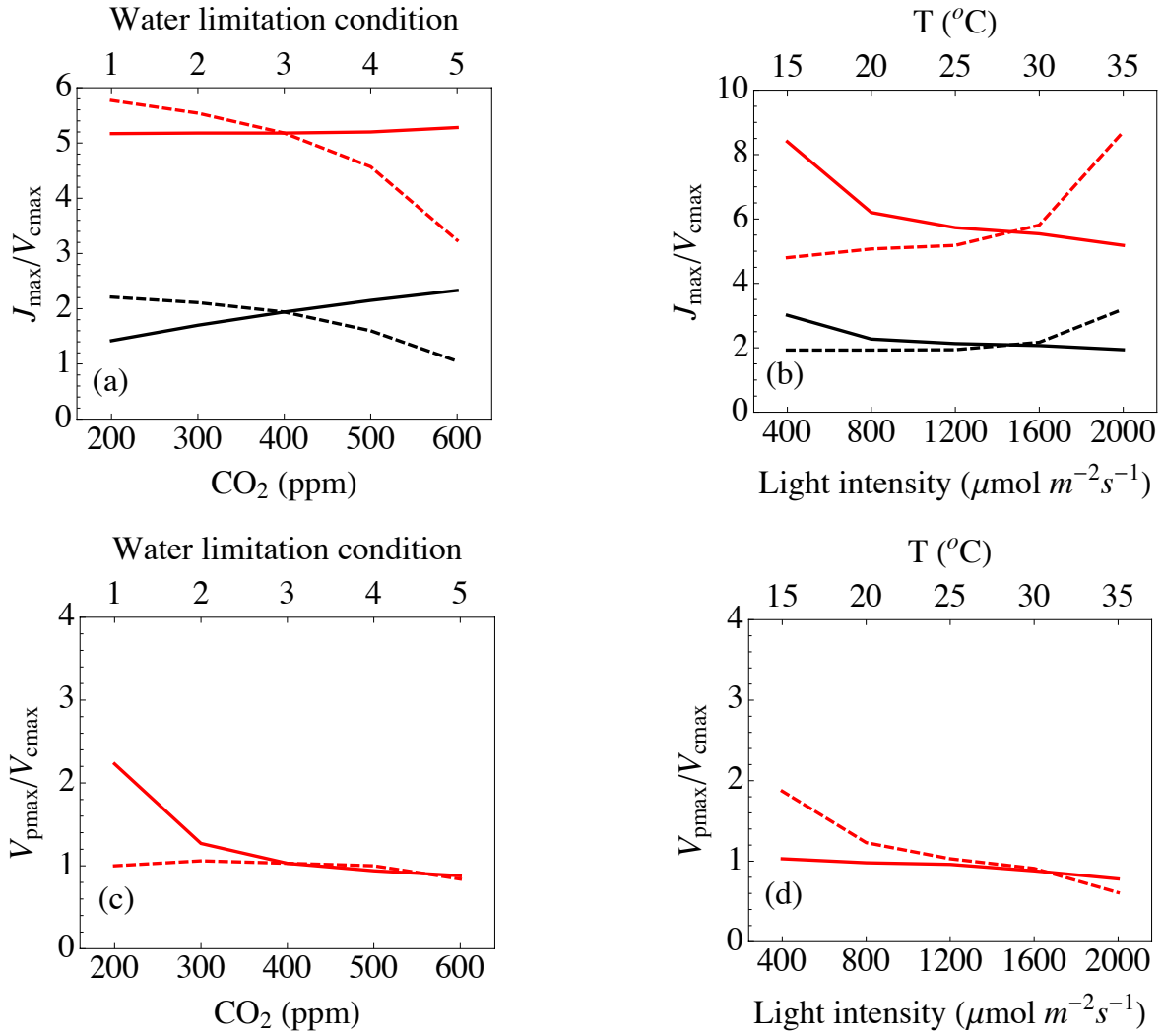
Fig. 7 Modeling results of optimal J_{max}/V_{cmax} and V_{pmax}/V_{cmax} for C_3 (black lines) and C_4 (red lines) under different environmental conditions. (a) Solid line: different CO_2; dashed line: different water limitation conditions (1: saturated water; 2: ψ_S=-0.5 MPa, VPD=0.625; 3: ψ_S=-1 MPa, VPD=1.25 MPa; 4: ψ_S=-1.5 MPa, VPD=1.875; 5: ψ_S=-2 MPa, VPD=2.5). (b) Solid line: different light intensities; dashed line: different temperature. Modeling results were obtained by controlling the other parameter at the in vivo measurement level.